J. Fluid Mech. (1981), *vol.* 110, *pp.* 73–95
Printed in Great Britain

On the growth of turbulent regions in laminar boundary layers

By MOHAMED GAD-EL-HAK, RON F. BLACKWELDER† AND JAMES J. RILEY

Flow Research Company, Kent, Washington 98031

(Received 2 September 1980 and in revised form 12 January 1981)

Turbulent spots evolving in a laminar boundary layer on a nominally zero pressure gradient flat plate are investigated. The plate is towed through an 18 m water channel, using a carriage that rides on a continuously replenished oil film giving a vibrationless tow. Turbulent spots are initiated using a solenoid valve that ejects a small amount of fluid through a minute hole on the working surface. A novel visualization technique that utilizes fluorescent dye excited by a sheet of laser light is employed. Some new aspects of the growth and entrainment of turbulent spots, especially with regard to lateral growth, are inferred from the present experiments. To supplement the information on lateral spreading, a surbulent wedge created by placing a roughness element in the laminar boundary layer is also studied both visually and with probe measurements. The present results show that, in addition to entrainment, another mechanism is needed to explain the lateral growth characteristics of a turbulent region in a laminar boundary layer. This mechanism, termed *growth by destabilization*, appears to be a result of the turbulence destabilizing the unstable laminar boundary layer in its vicinity. To further understand the growth mechanisms, the turbulence in the spot is modulated using drag-reducing additives and salinity stratification.

1. Introduction

The process of transition on a flat plate at zero angle of attack has been subjected to numerous intensive investigations. It was first studied by Burgers (1924), Van der Hegge Zijnen (1924), and in greater detail by Dryden (1934, 1936, 1939). Near the leading edge, the boundary layer is always laminar, provided there is no separation, and it becomes turbulent further downstream. Early theoretical work of Tollmien (1931) and Schlichting (1933) considered the initial growth of infinitesimal, two-dimensional disturbances superimposed on the laminar flow. When the Reynolds number exceeded a critical value, they found that the initial disturbance grew exponentially with time. The theoretically predicted growth rate was confirmed experimentally by Schaubauer & Skramstad (1948). Provided that all sources of external disturbance are sufficiently small, they showed that transition is preceded by the appearance of weak oscillations as predicted by the linearized theory of laminar instability. Those oscillations were initially in the form of two-dimensional instability waves with a wave speed about one-third of the free-stream velocity and a wave-

† Permanent address: Department of Aerospace Engineering, University of Southern California, Los Angeles, California 90007.

length several times the boundary-layer thickness. Klebanoff, Tidstrom & Sargent (1972) found that these waves rapidly developed three-dimensional aberrations culminating in a larger growth rate and the appearance of a velocity 'spike' before the flow broke down into turbulence.

Kovasznay, Komoda & Vasudeva (1962) mapped the region of concentrated vorticity in a boundary layer prior to breakdown. The total length of the region in which the vorticity exceeds the value obtained in a Blasius boundary layer was found to be approximately four times the boundary-layer thickness. Their results were consistent with the visualization study of Hama, Long & Hagarety (1957) which suggests that the amplification of small disturbances becomes associated at some stage with the concentration of vorticity along discrete lines, which subsequently distort into vortex loops within the boundary layer. The vortex loops themselves go through a process of distortion and extension, finally resulting in the breakdown into turbulence.

Since the three-dimensionality seems an important aspect of the growth of small disturbances, Gaster & Grant (1975) studied experimentally the formation and development of a wave packet generated in a laminar boundary layer on a flat plate. The packet was artificially generated by a short-duration acoustic pulse, which was injected through a minute hole on the plate. Their experimental results were compared with a linear model of a wave packet proposed by Gaster (1975). The comparison was quite good close to the source, but was not maintained far downstream, where the experimental packet showed various irregularities. The wave-crests of the propagating wave packet became distorted when the amplitude of the initial disturbance was large enough. These distortions of the wave fronts were associated with steep shear layers within the boundary layer, and with high-frequency bursts of oscillation that eventually led to embryo turbulent spots (Gaster 1978).

The appearance of turbulent spots within a laminar boundary layer had been first reported by Emmons (1951) who observed spots which were created randomly as the boundary layer underwent transition. On the basis of visual observation in a water table, Emmons concluded that randomly generated spots grow uniformly and act independently of one another as they are swept downstream by the flow. He developed a model which related some statistical properties of the spots to a single source-rate density function. Elder (1960) used dye to visualize the turbulent spots. He observed a point-like breakdown, in which the spots originate from a very small volume within the boundary layer. He investigated the conditions required for breakdown to turbulence, and the degree of interaction between adjacent spots. Elder concluded that breakdown is determined by local conditions, and is essentially independent of the Reynolds number and boundary-layer thickness. A critical Reynolds number is only required in order to amplify small disturbances, whereas sufficiently strong disturbances may burst into turbulence almost instantaneously regardless of the Reynolds number. Elder observed the interaction between two artificially generated spots which were displaced laterally, and concluded that there was no noticeable alternation in the growth rate of one spot owing to the presence of the other. Thus, he verified a major assumption in Emmons' model for the statistical properties of the spots.

Schubauer & Klebanoff (1956) continually initiated turbulent spots in a laminar boundary layer and measured the velocity signals and celerities associated with the

spot. They also reported a 'calmed region' immediately following the spot which was more stable than the surrounding flow.

Coles & Barker (1975) used conditional sampling techniques to study the spot's velocity field. By assuming a two-dimensional mean flow, they educed the streamline pattern in the centre of the spot and suggested that the spot grows not only by entraining irrotational fluid from the ambient free stream, but also by entraining fluid from the ambient laminar boundary layer.

Wygnanski, Sokolov & Friedman (1976) also used conditional sampling methods to obtain the average shape of a spot and the mean flow field in its vicinity. They found that fluid deep in the laminar boundary layer overtakes the rear interface of the spot, and is entrained into it. Fluid outside the boundary layer passes over the ridge of the spot and is entrained through the leading interface. Zilberman, Wygnanski & Kaplan (1977) extended the Wygnanski *et al.* work to track the structure of the turbulent spot as it merges and interacts with a turbulent boundary layer generated by a row of spherical trips. They showed that the spot structure tracked in the turbulent boundary layer retains its identity and suffers a negligible loss of intensity. The structure exhibits features in detailed agreement with those of the outer region of the turbulent boundary layer, such as a convection speed of $0{\cdot}9U_\infty$, and is consistent with existing two- and three-point space–time correlations.

Cantwell, Coles & Dimotakis (1978) conducted laser-Doppler velocity measurements for the flow in the plane of symmetry of a turbulent spot. Their measurements suggest that strong entrainment occurs along the outer part of the rear interface and also in front of the spot near the wall, while the outer part of the forward interface is passive. The experimental investigation of Wygnanski, Haritonidis & Kaplan (1979) in the region trailing the turbulent spot in a laminar boundary layer revealed the existence of a pair of oblique Tollmien–Schlichting wave packets. The breakdown of this ordered motion into a new turbulent spot was accompanied by the appearance of an intense shear layer inclined to the wall.

More recently, Van Atta & Helland (1980) conducted exploratory measurements of temperature fluctuations to study the structure of turbulent spots generated on a fully heated flat plate. They addressed a number of questions that have been raised by previous investigators regarding the mechanism by which a turbulent spot mixes the fluid in the boundary layer to transfer momentum and scalar properties during transition.

An important aspect of the turbulent spot, and indeed all such regions of localized turbulence, is the process by which the spot grows, incorporating previously non-turbulent fluid. In particular, near the plate the exterior fluid is rotational, and the lateral growth mechanism there might be different from classical entrainment. Charters (1943) was the first to note that the transverse growth rate of a turbulent region embedded in an unstable laminar boundary layer is significantly larger than usual turbulent entrainment rates. He called this process 'transverse contamination' and noted that it was independent of the originating cause. Corrsin & Kistler (1955) suggested that the spreading of a turbulent shear region into a shearing laminar region might be governed by a different propagation mechanism than that governing the spreading of turbulence into an irrotational fluid. They speculated that a destabilization of the already rotational flow could occur in addition to a transmission of random vorticity by direct viscous action (entrainment). Morkovin (1969) noted

that the transverse contamination process discovered by Charters (1943) has been the subject of only one further study, by Schubauer & Klebanoff (1956), who examined the turbulent wedge behind a roughness element placed in a laminar boundary layer.

Novel flow visualization techniques were used in the present study to investigate the structure and growth of a turbulent spot in vertical and horizontal planes. The spots were evolved in a laminar boundary layer on a nominally zero-pressure-gradient flat plate. Turbulent spots were initiated by a solenoid valve that ejects a small amount of fluid through a minute hole on the flat plate. The present visualization experiments were designed to clarify some of the above questions concerning turbulent spots. The processes by which the spot grows, incorporating the rotational fluid near the surface of the plate and the irrotational fluid outside the laminar boundary layer, were investigated. To understand the lateral growth mechanism better, turbulent wedges produced by introducing a roughness element into a laminar boundary layer were also investigated. Finally, the growth mechanisms were further studied by using drag-reducing additives and salinity stratification to modulate the turbulence in the spot or to change the laminar flow stability characteristics.

2. Experimental approach

2.1. *Towing tank system*

The flat plate used in the present experiment was towed at 40 cm s^{-1} through a towing tank that is 18 m long, 1·2 m wide, and 0·9 m deep. The flat plate was rigidly mounted under a carriage that rides on two tracks mounted on top of the towing tank. During towing, the carriage was supported by an oil film which insured a vibrationless tow, having an equivalent free-stream turbulence of about 0·1 per cent. The carriage was towed with two cables driven through a reduction gear by a 1·5 h.p. Boston Ratiotrol motor. The towing speed was regulated within an accuracy of 0·1 per cent. The main frame supporting the tank could be tilted and levelled by adjusting four screw jacks. This feature was essential for smooth operation of the carriage, whose tracks are supported by the main frame. The towing tank was designed so that flow visualizations can be made from the top, sides, bottom and ends. The bottom and side walls are made of 19 mm thick plate glass with optical quality. The end walls are made of 38 mm thick Plexiglas.

2.2. *Model and test conditions*

The flat-plate model used in the present experiment is sketched in figure 1. The arrow on this figure, and on all subsequent figures, indicates the flow direction relative to the plate. The flat plate was made of Plexiglas and is 191 cm long and 107 cm wide. The deviation of the plate from flatness is nowhere greater than 0·2 mm. Care was taken to avoid leading-edge separation and premature transition by having an elliptic leading edge and an adjustable lifting flap at the trailing edge. The flap was adjusted so that the stagnation line near the leading edge was located nearer the working surface.

Turbulent spots were initiated by a solenoid valve that ejected a small amount of fluid from a 0·5 mm diameter hole located 33 cm downstream of the leading edge. A square wave pulse having a 17 ms duration triggered the solenoid valve. The injected fluid created a three-dimensional disturbance, which evolved into a turbulent spot.

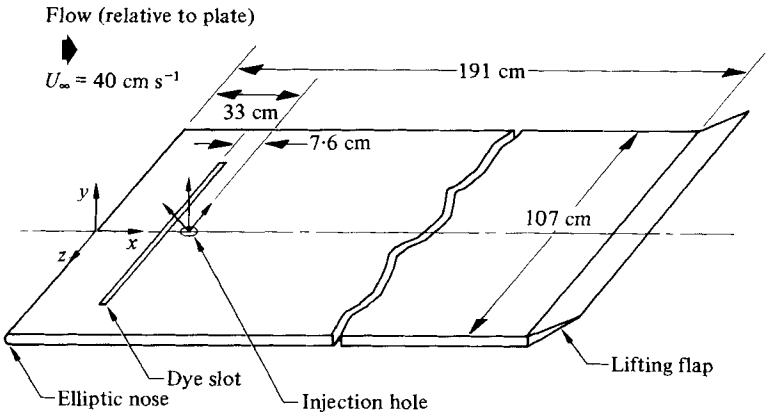

FIGURE 1. Schematic diagram of the flat plate and co-ordinate system.

The Reynolds number based upon a towing speed of 40 cm s^{-1} and upon the displacement thickness at the injection hole was 625, well above the critical Reynolds number for linear instability. Turbulent wedges were generated by placing a roughness element 30 cm behind the leading edge. The roughness element was a brass cylinder with 0·32 cm diameter and 0·25 cm height, placed with its axis perpendicular to the flat plate. When not disturbed, the boundary layer on the working surface remained laminar until tripped close to the trailing edge. The plate was positioned 5 cm from the tank walls and the circulation around the plate generated by the flap was such that disturbances were not communicated from the bottom surface to the top (working) surface.

2.3. *Flow visualization*

The turbulent regions were made visible by novel techniques which utilized fluorescent dye, i.e. dye which is visible only when excited by a strong light source of the appropriate wavelength. This provided an extra degree of freedom in observing the flow because both the dye and light location could be controlled within the limitations of the experimental apparatus. A 5 watt argon laser (Spectra Physics, Model 164) was used with a cylindrical lens to produce a sheet of light that could be projected perpendicular to each of the three axes as required. The light sheets were approximately 1 mm thick, which was sufficient to resolve the large structure within the turbulent regions.

Three different methods of dye injection were employed. In the first, a dye sheet seeped into the laminar boundary layer through a 0·15 mm wide, 30 cm long spanwise slot located 25 cm downstream of the leading edge. The slot was milled at a 45° angle inclined towards the trailing edge to minimize the flow disturbance. The slot was divided into four separate sections, each with its own dye source, so the spanwise mixing and diffusion of turbulent fluid could be studied. The dye remained on the plate surface until the turbulent spot caused it to lift and diffuse.

Discrete lines of dye could be allowed to seep into the laminar boundary layer by masking the spanwise slot with 32 cm long strip of electrical tape, in which thirty longitudinal slots, 1 cm apart and 0·5 cm long, were cut with a surgical knife. The resulting dye lines were less than 0·5 mm wide near the trailing edge of the plate.

Dye was also placed in the flow field by laying several thin, horizontal sheets prior

to towing the plate.† These layers remained thin, about 1 mm in thickness, due to the inhibition of vertical motion caused by introducing a weak saline stratification in the tank. Fluorescein, Rhodamine-B, and Rhodamine-6G dyes were used which fluoresced green, dark red and yellow, respectively, when excited by the argon laser. In a flood-light, the first two dyes fluoresced green and dark red, while Rhodamine-6G had a faint red colour. The alternating sheets of different colours remained quiescent until disturbed by the turbulent spot on the towed plate. The motion of the potential flow could also be observed since dye layers existed in the potential region also.

The visualization information was obtained using 35 mm photographs and 16 mm ciné films. The cameras were typically controlled by microswitches which filmed the spot at predetermined times after its generation. The 16 mm films were analysed by a stop-action projector.

2.4. *Stratification and polymer additives*

A stratified fluid of a predetermined density profile could be made by feeding salt water, layer by layer with increasing density, into the tank through two channels along the tank bottom. The salinity of the water and its feeding rate determined the density profile in the undisturbed tank. A linear density profile is characterized by its Brunt–Väisälä frequency N, defined as

$$N \equiv \frac{1}{2\pi}\left(\frac{-g}{\rho_0}\frac{d\rho}{dy}\right)^{\frac{1}{2}},$$

where g is the gravitation acceleration, ρ_0 is a reference density (1 g cm^{-3}), and $\rho(y)$ is the undisturbed density profile.

The Brunt–Väisälä frequency provides a convenient measure of the time scale at which stratification effects are important. It is the natural frequency of oscillation of a fluid particle under infinitesimal perturbation. In the present experiment, N varied in the range 0–0·7 Hz.

The polymer used in the present experiment was Polyox, WSR-301 (polyethylene oxide) manufactured in powder form by Union Carbide Corporation. It has a molecular weight of about 4×10^6, and was used in concentration of 50 parts per million (p.p.m.) by weight. A uniform dispersion of the Polyox resin in the towing tank water was necessary for good dissolution. If the resin powder was not properly dispersed, the partially dissolved, wetted particles agglomerated and formed gels which would dissolve only with prolonged high-speed agitation. However, such prolonged high-speed agitation must be avoided to prevent shear degradation of the resin. A novel method was used in the present study to dissolve the polymer in the water. An aspirator driven by 80-psi compressed air was used to lift the dry polymer powder from its container into a 25 mm PVC pipe. The pipe released the mixture of air and polymer near the bottom of the towing tank. The air provided an ideal medium for dispersing the resin. The polymer mixed well with the water without forming gels, and the air escaped to the surface.

† This technique was originally developed by H.-T. Liu and J.-T. Lin at Flow Research.

3. Results and discussion

3.1. *Spot structure*

Several reference runs were made to check the overall quality of the towing system and the established flow field. Conventional food-colouring dye was allowed to seep from the spanwise slot and several holes near the leading edge. Dye seeping from the leading-edge holes indicated that the stagnation point was slightly toward the working side of the plate and no separation occurred. When unperturbed, the dye from the slot remained on the surface and had a glassy smooth appearance over the entire length of the plate, indicating that a laminar boundary layer was maintained until the end of the plate, where the Reynolds number was $U_\infty x/\nu = 7{\cdot}6 \times 10^5$ for a towing speed $U_\infty = 40$ cm s^{-1}. When disturbed by the solenoid injection of fluid through the hole at $x = 33$ cm, a spot having the classical arrowhead shape could readily be observed as the turbulence removed the dye from the wall layer. The developing shape of several spots was mapped to determine the virtual origin. It occurred at $x = 43 \pm 2$ cm, i.e. 10 cm downstream of the ejection hole, and at $t = 0{\cdot}63 \pm 0{\cdot}1$ s after the ejection.

A plan view of the turbulent spot moving from left to right (relative to the plate) is shown in figure 2 (plate 1). The fluorescent dye was injected uniformly through the spanwise slot, and was made visible by a sheet of laser light located at $y \simeq 0$. As the spot developed, the turbulent motion in the spot removed dye from the wall and elevated it above the plate. Since the light sheet was slightly thicker than the dye layer on the plate, both the dye in the laminar boundary layer and the dye near the wall within the spot were visible. The light illumination was from both sides of the figure. Some absorption of the light occurs and consequently the sheet loses intensity in the spanwise direction, so that the sides appear brighter than the interior. The general arrowhead shape of the spot is clearly evident. Some evidence of the streamwise streaky structure at the rear of the spot is seen in the figure. However, since little dye remained at this elevation after the passage of the spot, the streaks were more easily seen using conventional floodlights which provided an integrated view and hence more contrast. This suggests that the streaks are made visible by sweeping the dye into thin sheets in the x, y plane, consistent with the concept of counter-rotating streamwise vortices discussed by Cantwell *et al.* (1978).

One feature which was especially noticeable at this elevation is the bright dyed regions following the spot which appear behind the wing tips and form an apex approximately one spot length behind the trailing edge. The ciné film revealed that the dye in this region had seeped into the area originally scoured by the spot during its passage. As the dye seeped into the region it seemed to coalesce into streaks as seen. To be so brightly illuminated, the dye must have been lifted above the surrounding dye fluid in order to have received a higher-intensity excitation from the sheet of laser light. The evidence suggests that the counterrotating vortices extend into this region and aggregate the dye into streaks, lifting it up in the process.

Several runs were taken using different elevations of the sheet of light. As the height of the sheet increased, individual turbulent eddies inside the spot became more discernible and their length scales in the streamwise and spanwise directions increased. A sequence of views of the spot in the x, z plane is shown in figure 3 (plate 2). The height of the light sheet was 1·3 cm above the plate, making the height almost twice

the undisturbed laminar boundary-layer thickness at this location ($\delta_l \simeq 0{\cdot}7$ cm). The elapsed time since the spot was generated is shown on the right, and for reference a scale of the physical dimensions is shown. Some turbulence may exist between the dyed nodules seen in the figure, since the dye tags only fluid which was originally near the wall. Nevertheless, this sequence and films of the x–y cross-section of the spot (see figure 5) clearly show well-mixed turbulent eddies moving away from the wall. Most striking is that, at this elevation, the growth occurs at the rear of the spot with very little new turbulence appearing near the head. That is, first several turbulent eddies appeared. As the flow field developed, it was apparent that these eddies were near the head of the spot and they remained relatively coherent until swept from the field of view. At this elevation, the spot grows by the appearance of more eddies as seen in the figure. However, the new eddies typically occur only upstream of the existing ones, i.e. towards the trailing edge of the spot. Since the outer irrotational fluid was not marked with dye, this sequence cannot be used to determine how entrainment of non-vortical fluid occurs. However, it is clear that the observed eddies originated nearer the wall and were moving outward. There was a slight tendency for the turbulent eddies to appear first near the wingtips and later in the middle of the spot. This may have been a manifestation of the visualization technique, since the earlier passage of the head of the spot would have left less dye for tagging the turbulence in the interior. The length scale in the streamwise and spanwise directions of the turbulence eddies within the spot at this elevation was roughly a turbulent boundary-layer thickness.

The ingestion into the spot of vortical laminar fluid near the wall is seen in figure 4 (plate 1). In this run, discrete lines of fluorescein dye seeped through the tape-covered spanwise slot and occupied the wall region of the laminar boundary layer. A sheet of laser light at $y \simeq 0{\cdot}1$ cm illuminated the turbulent spot as well as the dye lines in the surrounding laminar flow. The narrow dark region perpendicular to the dye lines and crossing the spot in figure 4 was due to a shadow from the plate support. The leading edge of the spot in this figure was 50 cm downstream of the ejection hole. As the spot overtook the dye lines, large-amplitude motions were observed along each dye line. The streamwise scale of the distortions evidenced by the dye lines was approximately 1 cm compared with the laminar boundary-layer thickness of approximately 0·7 cm.

In the ciné films, the disturbances often appeared wave-like because 1–3 regularly spaced motions could be observed along a given dye line. In this view, a two-dimensional wave would be visible only if it had a velocity component along its crest to distort the dye line. Thus, if the observed motion is a wave, it must be oblique. In addition, it must be quite narrow because no obvious correlation of the motion from one dye line to the next could be consistently observed. A point of constant phase on each wave-like structure was observed to move downstream at roughly $0{\cdot}4U_\infty$–$0{\cdot}5U_\infty$, and hence was rapidly overtaken by and ingested into the spot. These disturbances might have existed even further ahead of the spot, but were not visible until their amplitude became sufficiently large. The fluctuations observed in figure 4 are similar to those seen in the photographs of Cantwell *et al.* (1978) and Falco (1977). Although their techniques were different, they found sinuous motions upstream of the leading edge of the spot. These fluctuations were best seen in the present study when the light sheet was at approximately $0{\cdot}2\delta_l$. In the film from which figure 4 was extracted, an earlier sequence illustrated a strong spanwise velocity near the wingtip. As the

spot continued to expand outward, the dye line closest to the wingtip was also moved outward in agreement with the spanwise velocity component measured by Wygnanski *et al.* (1976).

A different means of visualizing the spot is shown in figure 5 (plate 3). The pre-existing horizontal dye sheets were illuminated primarily by the light sheet in the x–y plane; however, the dye also reflected some room lighting. On the original films and photos, this room-lit dye provided a convenient reference line from which the disturbed motion could be compared. The sheet of light could be placed at different spanwise locations, providing cross-sections of the spots at different z-positions. The example in figure 5(*a*) is taken on the centre-line, and figure 5(*b*) is taken at 6 cm (approximately $10\delta_l$) off centre. The outline of the spot in this view is highly contorted at all spanwise locations. The general shape and aspect ratio of the spot agrees with the conditionally averaged shape of Wygnanski *et al.* (1976) and Cantwell *et al.* (1978). However, no single dominate eddy was observed at any spanwise location. Instead the spot contained many eddy structures having length scales of typically a turbulent-boundary-layer thickness δ_t. As seen in the figure and in the ciné-film frames from which it was extracted, they have a preferred inclination in the downstream direction. These eddies seemed to be independent of each other; in fact, the interior of the spot at all spanwise locations resembled a turbulent boundary layer. The eddies slowly grew and moved away from the plate, thus providing the growth in the normal direction as observed in figure 3.

The different colours in the dye layers allowed one to observe the turbulent entrainment and mixing in some detail. Most of the observable entrainment occurred on the back of the spot, as reported by Cantwell *et al.* (1978). Although some care must be exercised in drawing conclusions about entrainment based upon data in one plane, the most obvious mechanism of entrainment observed seemed to be 'gulping', i.e. large parcels of irrotational fluid being ingested into the boundary layer between two eddy structures. Examples of this are seen in figure 5 where the potential fluid extends deep inside the turbulent region. Similar conclusions have been drawn by Falco (1977) for a fully developed turbulent boundary layer at moderate Reynolds numbers. The other mechanism of entrainment, i.e. 'nibbling', may be important for length scales smaller than those shown in the figure.

The effects of the spot are felt over a large domain in the irrotational region. For example, even though the outermost dye layer in figure 5(*a*) is located at $2\delta_t$, it is observed to have been displaced at least 0·5 cm ($0{\cdot}2\delta_t$) as the spot passes underneath. This fact is consistent with the strong correlation of the normal velocity component extending into the potential region which was reported by Blackwelder & Kovasznay (1972) in a turbulent boundary layer. In front of the nose, the dye lines at $y \simeq \delta_t$ have been displaced downward, indicative of the strong normal velocity component reported by Wygnanski *et al.* (1976). Closer to the turbulent eddies, stronger distortions are observed as the irrotational fluid is marked for entrainment.

Figure 6 (plate 4) shows two cross-sectional views in the x–y plane of the turbulent spot. The fluorescent dye was allowed to seep from the spanwise slot and occupy the wall region as in figures 2 and 3. The dye was excited with a sheet of light in the x–y plane at $z = 0$ (figure 6 *a*, close-up lens used), and $z = 6$ cm (figure 6 *b*). In the ciné-film frames from which each view was taken, a most interesting phenomenon was observed to occur consistently. As obtained from the ciné film and sketched in figure 7, the

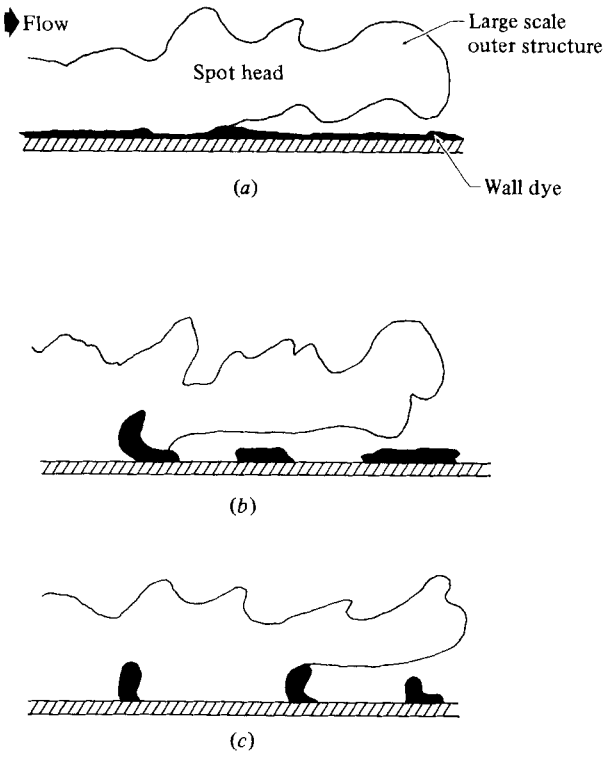

FIGURE 7. Sketch of events preceding the break-up of wall dye. (a) Large-scale outer structure moving over wall dye layer. (b) Wall dye is separated into lumps with regular spacing. (c) The lumps are removed from the wall along similar trajectories.

turbulence near the head of the spot does not extend all the way to the wall in agreement with the velocity measurements of Cantwell *et al.* (1978) and Wygnanski *et al.* (1979). This region appears to have been swept over the slower laminar flow near the wall, producing a large overhang of the spot's leading edge. Initially, the dye lying on the wall is relatively undisturbed, in spite of the existence of large-scale turbulent structures one laminar boundary-layer thickness δ_l above it. At later times, the wall dye begins to show signs of disturbance. It first separates into several lumps, possibly due to a strong vertical velocity component. The discrete regions of dye seem to have a particular 'wavelength' of approximately one or two laminar boundary-layer thicknesses at this location. This is consistent with the motion shown in figure 4. At still later time, the wall dye is removed and mixed into the spot, without any apparent entrainment occurring. The resulting characteristic pattern of the dye suggests that it may be associated with a definite type of vortex motion.

A cross-section of the spot in a plane perpendicular to the mean flow is shown in figure 8 (plate 5). The flow (relative to the plate) is out of the plane of the figure. Although the laser sheet was aligned in the y–z plane, the camera was by necessity outside the towing channel; thus the view is from a 45° oblique angle and the horizontal scale is contracted by about 30 per cent. The view in figure 8 is approximately halfway between the nose and tail of the spot. The spot again appears to be composed of a random collection of turbulent eddies as illustrated by figures 3 and 5. The most impressive feature from this angle was a strong motion perpendicular to the wall

which can be inferred from the dye-line displacement slightly outside the spot. In the irrotational region, the effects of a motion toward the wall are seen directly above the side of the spot. A little further out in the spanwise direction, a large upward displacement is observed in the laminar boundary layer. Wygnanski *et al.* (1976) measured the normal velocity at $y/h_0 = 0{\cdot}3$ (h_0 is the nominal maximum height of the spot). They observed a component toward the wall at the edge of the spot, but did not make measurements in the vicinity of the positive normal velocity.

Careful viewing of the movie sequence from which figure 8 was extracted revealed no strong evidence of a single predominant vortical structure. The local dynamics within the spot seemed to be controlled by individual, independent eddies, similar to those within a turbulent boundary layer.

3.2. *Lateral growth*

One interesting and important aspect of the turbulent spot is the process by which it grows, incorporating previously non-turbulent fluid. From the previous discussion and the work of others, e.g. Wygnanski *et al.* (1976) and Cantwell *et al.* (1978), it is apparent that the spread of the spot normal to the plate is mainly due to classical entrainment, in much the same way that a turbulent boundary layer entrains previously irrotational fluid. This process was first studied in detail by Corrsin & Kistler (1955) in typical turbulent shear flows. Some of the most distinctive features of the classical concept of entrainment (see Townsend 1976) are:

(1) The turbulent region is separated from the non-turbulent region by a distinct interface. Corrsin & Kistler (1955) speculated that the interface thickness is of the order of the Kolmogorov length scale, $(\nu^3/\epsilon)^{\frac{1}{4}}$.

(2) The turbulent region is characterized by random three-dimensional vortical flow; the non-turbulent fluid is irrotational. Thus the process of entrainment must ultimately be by direct contact, i.e. by the local diffusion of vorticity. This is followed by a rapid increase in vorticity due to local straining.

(3) If a passive scalar is introduced into an entire turbulent region, it will also mark new fluid acquired by entrainment because of the turbulent mixing (e.g. Fiedler & Head 1966; Chen & Blackwelder 1978).

There is strong reason to believe that the turbulent spot does not spread parallel to the plate by classical turbulent entrainment. First of all, the fluid exterior to the spot in the laminar boundary layer is highly rotational. Therefore, feature 2 above does not hold, and it is not necessary that the turbulent region spread through direct contact. Secondly, the fluid within the laminar boundary layer is unstable, suggesting the possibility of another mechanism.

Some support for the speculation that the spot grows by different mechanisms in the two directions is obtained by examining the growth rates in the normal and spanwise directions. Let h denote the characteristic scale in the direction perpendicular to the wall. Cantwell *et al.* (1978) have found that h grows linearly in the spot, very close to the growth of h in a turbulent boundary layer. Using their similarity transformation, the growth rate of h is $dh/dx \simeq 0{\cdot}013$. On the other hand, the growth rate of the characteristic scale in the spanwise direction, b, can be estimated from the maximum angle subtended by the spot measured from its virtual origin. Using the typical value of 10° as reported by Wygnanski *et al.* (1976), yields $db/dx \simeq 0{\cdot}18$. Thus the spanwise growth is more than an order of magnitude greater than the

classical entrainment growth in the normal direction, suggestive of an additional mechanism.

A series of visualization experiments were performed to elucidate the lateral growth mechanism. Dye was used as a passive scalar contaminant to mark the initially turbulent fluid. If turbulence were only acquired by entrainment, the dye would continue to diffuse and mark the entire turbulent region analogous to the smoke and to the heat used respectively by Fiedler & Head (1966) and Chen & Blackwelder (1978). Alternatively, if additional turbulence were acquired by mechanisms other than classical entrainment, the spot would not all be dyed. In one experiment, blue dye was injected from the solenoid valve in order to mark the initial patch of turbulence, and red dye was emitted through the slot in order to mark all the turbulence within the spot. Movies of the plan view of the turbulent spot indicated that the original turbulent region, dyed blue, did not spread nearly as fast as the spot. In other words, new turbulent fluid was incorporated into the spot without being tagged with blue dye. This is in contrast to classical entrainment as exemplified by feature 3 above.

To further explore the diffusive properties of the spot, the dye slot was partitioned into four independent regions, and different dyes were used in each slot.† The ciné records clearly showed that the spanwise diffusion of dye across the sections is much less than the spanwise growth rate of the spot. Estimates of the dye diffusion obtained from the films indicate that the spanwise diffusion was comparable to diffusion in the normal direction.‡ Although the diffusion of dye proceeds at the same rate as entrainment in the normal direction, diffusion and spot growth have markedly different rates in the lateral direction. Townsend (1976) points out that the entrainment rate of a turbulent boundary layer is much less than that of a jet or wake, so that one could argue that the classical entrainment mechanism with different rates could account for the contrasting growth rates in the normal and spanwise directions. In the classical concept of entrainment, however, diffusion and entrainment proceed at the same rate, and the present experiment clearly shows that the lateral diffusion of the dye within the spot is significantly different than the turbulence growth rate in that direction.

3.3. *Wake of a roughness element*

To examine further the nature of the spread of a turbulent region into an unstable, laminar boundary layer, the turbulent wake behind a roughness element in a laminar boundary layer was studied. The roughness element, a circular cylinder with 0·32 cm diameter and 0·25 cm height, was placed 30 cm behind the leading edge, and the plate was towed at 30 cm s^{-1}. The wake from the roughness was easily visualized by coating it with red dye dissolved in corn syrup, as seen in figure 9(*a*) (plate 6). Figure 9(*b*) was taken under identical conditions except blue dye was seeped through the spanwise slot. Conventional floodlights were used to illuminate the dyes, resulting in an integrated view of the flow field. As is readily evident, the turbulence region, which is marked by the dye seeping from the slot, extends significantly outside the wake of the roughness element, which is marked by the dye pasted on the roughness. The width of the turbulent region increased more rapidly and was always wider than the wake of the

† This technique was originally suggested by M. Morkovin.

‡ The diffusion rates in the lateral and normal directions in a turbulent boundary layer are also known to be comparable.

object initiating the wedge. In the film from which figure 9(*b*) was obtained, an occasional spot could be observed moving downstream. It was distinguishable from the other turbulence because its wingtips extended slightly beyond the region marked by the turbulent dye. The half-angle of spread of the wake in figure 9(*a*) is approximately 2°, whereas the total turbulent region marked by the dye seeping from the spanwise slot grows at $6 \pm 0{\cdot}5°$. The outer region of the observed wingtips subtended a half-angle of $10 \pm 0{\cdot}5°$. Similar data have been obtained by Schubauer & Klebanoff (1956) using hot-wire measurements. Klebanoff (private communication) observed that, as the Reynolds number increased, the growth rate of the total turbulent region behind the roughness element approached that of the turbulent spots.

When the roughness element was removed and the plate towed at the same velocity, the boundary layer remained laminar over the entire surface. When the plate was towed at slow enough speed the roughness was located in a laminar boundary layer which was stable according to the linear theory ($U_\infty \delta^*/\nu < 420$), flow irregularities introduced by the cylinder were damped and no turbulent wedge was observed. Apparently not just a vortical flow, but an unstable vortical flow is a necessary condition for the lateral growth process to take place.

The above visualization experiments confirm that the augmented spanwise growth of a turbulent region embedded in an unstable laminar boundary layer is not by classical entrainment, but is probably due to a destabilization process, in which the turbulent eddies inside the spot or wedge induce such a strong disturbance that the surrounding laminar flow breaks down. This destabilization process may be closely related to the wave-like structures shown in figures 4, 6 and 7. It would furthermore be expected that the properties of the turbulent–nonturbulent interface are different from those in the classical entrainment case.

In order to obtain more quantitative information on the difference between the roughness wake and the entire turbulent region, a limited amount of data were taken in an air flow using the wind tunnel and experimental flat plate described by Wygnanski *et al.* (1979). A single roughness element located on the centre-line of the flat plate 60 cm from the leading edge was used to generate a turbulent wedge. The roughness element was a single ceramic 1·8 mm diameter cylinder extending 3·7 mm from the plate. The cylinder was wrapped with 0·05 mm nichrome wire having a total resistance of 6·2 ohms. During the experiment the nichrome wire was heated by applying a 6 volt electrical supply across it, producing an estimated surface temperature on the cylinder of approximately 150 °C. All of the data were taken with a free-stream velocity of 1000 cm s^{-1}. The Reynolds number based upon the displacement thickness at the roughness element was 1090, so the cylinder was located in a highly unstable laminar boundary layer.

The temperature wake and the turbulent wedge were explored downstream by using a single hot-wire traversed in the spanwise, z, direction up to 80 cm downstream. The hot-wire was held at a fixed position of $0{\cdot}8\delta^*$ above the plate by using a small sled similar to that employed by Anders & Blackwelder (1980). The wire was first driven by a constant-temperature hot-wire anemometer having an overheat of 1·25 in order to measure the velocity profile. A second trajectory along the same path was taken with the wire driven by a constant-current anemometer having a 1·005 overheat to study the thermal wake. The anemometer signals and the voltage proportional to the spanwise location of the traverse were digitized and stored on

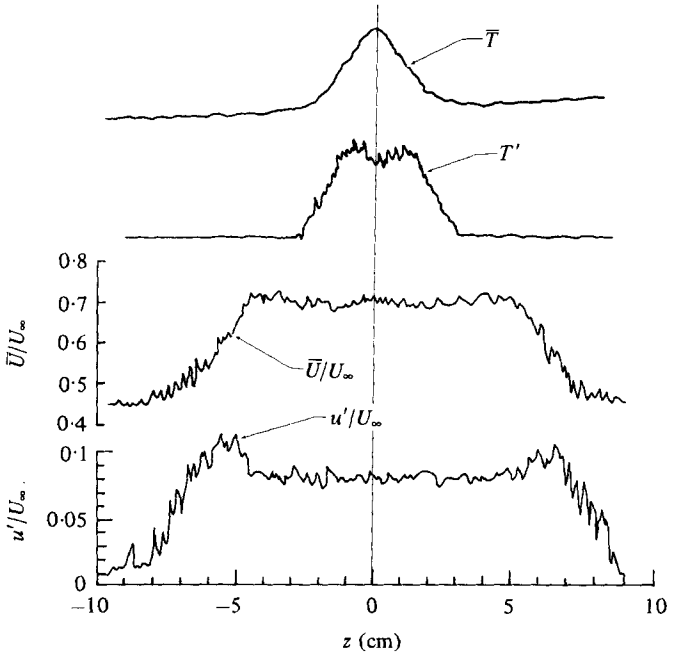

FIGURE 10. Spanwise profiles of the mean and fluctuating temperature and velocity at $y/\delta^* = 0{\cdot}8$, 60 cm downstream of the heated roughness element. The temperature scales are arbitrary.

magnetic discs under the control of a DEC 11/55 digital computer. The mean and r.m.s. temperatures and velocity profiles were computed and plotted on a Tektronix 4010 computer terminal.

Spanwise traverses were taken every 10 cm downstream of the roughness element up to a maximum of $\Delta x = 80$ cm. A typical example of the output is shown in figure 10 for $\Delta x = 60$ cm. It is readily apparent that the temperature and velocity profiles have a significantly different structure. At all streamwise locations, both the mean and fluctuating signals indicated that the temperature wake was much narrower than that marked by the velocity. The width of the thermal wake and the total width of the turbulent wedge were defined at each downstream position by finding the spanwise location where the profile obtained one half of its maximum value. The results for the fluctuating temperature and velocity signals are seen in figure 11. The corresponding widths for the mean velocity and temperature were also computed and they had a behaviour similar to those shown by the fluctuating quantities in the figure. After equilibrium growth rates were established approximately 10–20 cm downstream from the roughness element, two different growth rates were readily apparent. The thermal wake at this Reynolds number grows with a nominal spreading rate having a half-angle of 1·3°; however, the turbulent wedge, as defined by the fluctuating velocity signals, grows with a corresponding half-angle of 8°.

Schubauer & Klebanoff (1956) also studied the fluctuating velocities found downstream of a single roughness element in an unstable laminar boundary layer. They reported measurements of the turbulent–nonturbulent interface associated with the wedge behind a roughness element located at $U_\infty x/\nu = 9{\cdot}5 \times 10^5$. Their fully turbulent region grew with a half-angle of 6·4° and the intermittency extended out to an angle

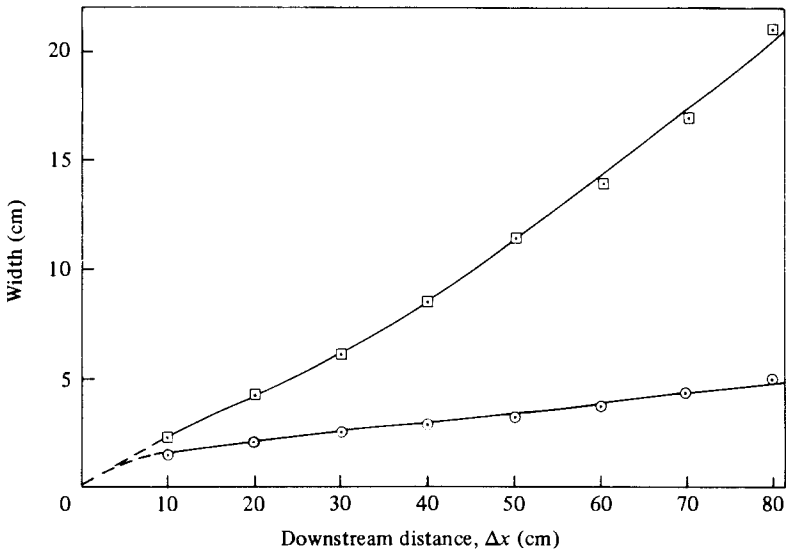

FIGURE 11. Growth of the thermal wake and the turbulent wedge as determined by the widths of the fluctuating temperature and velocity profiles. ⊡, Velocity; ⊙, temperature.

of 10·6°, consistent with the above results. Similar results were reported by Meyer & Kline (1961) who also observed that the turbulence within the wall layer within the turbulence wedge was similar to that in a fully developed turbulent boundary layer.

Another interesting observation obtained from the spanwise traverses such as shown in figure 10 is that the fluctuating velocity profile always had a distinct maximum near the edges of the turbulent wedge. These peaks always appeared in the regions where the flow was intermittently laminar and turbulent and may be due to the intermittency in the signal at this location or may include more energetic fluctuations there. This corresponds to the regions where $\overline{U}/U_\infty$ is midway between its laminar and turbulent values in figure 10.

3.4. *Effects of drag-reducing polymers*

In an effort to shed some light on the growth mechanisms of turbulent regions in laminar boundary layers, drag-reducing additives were used to modulate the growth rates. Polyox, WSR-301 polymer, was used in a concentration of 50 p.p.m. The flat plate was towed at 40 or 60 cm s^{-1}, corresponding to R_{δ^*} at the injection hole of 625 or 766, respectively. The mean wall strain rate in the turbulent spot ranged from 325 to 570 s^{-1} for a towing speed of 40 cm s^{-1}, and 670 to 1210 s^{-1} for the higher towing speed. These values are higher than the onset strain rate for observable drag reduction for WSR-301, which is about 320 s^{-1} (Berman & George 1974).

Figure 12 (plate 7) shows a plan view of a turbulent spot generated in pure water and one generated in a dilute polymer solution. Each spot is moving from left to right relative to the plate, which is towed at 40 cm s^{-1}. Fluorescent dye was injected uniformly through the spanwise slot, and was made visible by a sheet of laser light located at $y = 3$ mm. As each spot developed, the turbulent motion removed dye from the wall and elevated it above the plate. Less dye seemed to have been removed from the plate

when using polymer, since the spot in figure 12(*b*) is fainter than that in figure 12(*a*). This seems to indicate that the turbulence intensity in the lower region of the spot is reduced when using polymers. In the ciné-film frames from which figure 12 was extracted, one can observe that the polymer tends to suppress the small-scale turbulent structures. Also, with the polymer additive, the lateral growth rate is reduced by about 15 per cent, resulting in a more elongated spot in the dilute polymer solution. This reduction is much less pronounced than the 40 per cent reduction observed by Bertshy & Abernathy (1977). It should be noted, however, that the wall strain rate in their experiment was about an order of magnitude higher than that in the present study. Moreover, because their experiments were carried out using a shallow water table, their flow extended only to y^+ on the order of 100, and polymer effects could conceivably be more pronounced in the absence of outer flow. The addition of the polymer does not seem to affect significantly other gross parameters, such as the propagation speed of the head or the tail of the spot.

One interesting result of previous experiments on turbulent spots is that, for non-accelerated flat-plate boundary layers, the average shape of the spot appears to be independent of ambient conditions, i.e. local Reynolds number and hence strain rate, at least for the range of experiments to date. Thus the lateral angle subtended by the spot has always been found to be approximately 10°, and the growth rate normal to the wall to be approximately that of a turbulent boundary layer. However, when the polymer is added, the lateral growth rate appears to depend on the strain rate (and on the polymer concentration), as found from comparing our results with those of Bertshy & Abernathy (1977).

Figure 13 (plate 5) shows another plan view of a turbulent spot generated in the dilute polymer solution. The plate was towed at 60 cm s^{-1}, and the sheet of laser light was located at $y \simeq 0$. The darkened region directly upstream of the head is caused by structural beam partially blocking the sheet of laser light. The average eddy size is smaller than that depicted in figure 8, because the cut is closer to the wall and because the Reynolds number is higher. The wall strain rate in this case is about 20 per cent higher than that in figure 12.

Several runs were taken using different elevations of the sheet of light. As the height of the sheet increased, individual turbulent eddies inside the spot became more discernible, and their length scale in the streamwise and spanwise directions increased. The polymer decreased the spanwise growth rate 15 per cent at all elevations.

The effect of the polymer on the vertical growth of the spot was minimal. Thus, it seems that the addition of polymer mainly affects the spanwise growth of a turbulent spot. This is consistent with the concept of the spot growing vertically by classical entrainment, but growing laterally by destabilization. It is known that drag-reducing effects associated with polymers occur in regions of high strain rate, e.g. near boundaries, suppressing smaller-scale motions. Thus it is likely that the stability characteristics of the laminar boundary layer are modified by the drag-reducing additives, i.e the flow is less unstable. Hence the destabilization process is somewhat inhibited, resulting in a slower lateral growth rate. A better understanding of the dependence of lateral growth rate on the local strain rate, and a determination of the effects of the polymers on the stability characteristics of the flow should thus give further insight into this lateral growth mechanism.

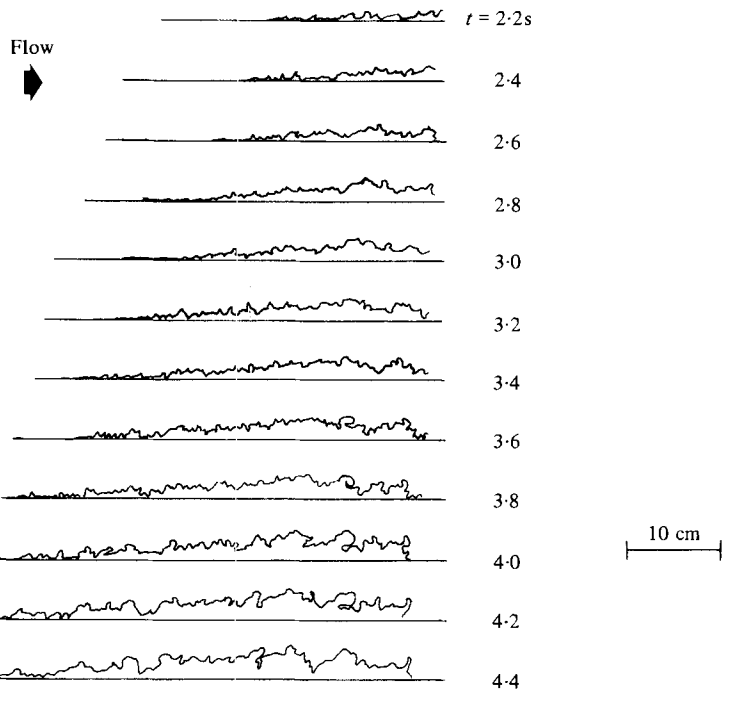

(*a*)

FIGURE 15. Traces from ciné film frames showing cross-sectional view of an evolving turbulent spot; $z = 0$, $U_\infty = 40$ cm s^{-1}. (*a*) Homogeneous fluid. (*b*) Stratified fluid, $N = 0{\cdot}1$ Hz.

3.5. *Stratification effects*

Stratification effects were used to further modulate the growth mechanisms in turbulent regions. Turbulent spots were generated in the presence of a linear, stable density gradient having a Brunt–Väisälä frequency in the range 0–0·7 Hz. Figure 14 (plate 8) shows the effects of stratification on the vertical growth of a turbulent spot. The fluorescent dye was illuminated by a sheet of laser light in the x–y plane, located at $z = 0$. The plate was towed at 40 cm s^{-1}, and both spots are 3·5 seconds old. Figure 14(*a*) shows the spot in the homogeneous fluid ($N = 0$), and figure 14(*b*) shows the spot in the stratified fluid ($N = 0{\cdot}1$ Hz). The stratification inhibits the vertical growth of the turbulent spot. The effect is more pronounced near the head of the spot (to the right). This is expected since the head of the spot is generated first, and thus has more time to 'feel' the stratification effects. The vertical turbulent motion causes vertical transport of mass, which in turn converts kinetic energy to potential energy. As a result, vertical motion is suppressed and the vertical mass transport weakens.

Figure 15 shows a series of traces taken from ciné-film frames. Run conditions were the same as that in figure 14. Figure 15(*a*) shows a cross-sectional view in the x–y plane of a turbulent spot evolving in a homogeneous fluid, while figure 15(*b*) shows a similar view for a spot evolving in a stratified fluid with a Brunt–Väisälä frequency 0·1 Hz. The elapsed time since the spot was generated is shown on the right, and for reference a scale of the physical dimensions is shown. The head of the spot in the stratified flow began showing evidence of 'collapse' at $t = 2{\cdot}6$ seconds ($Nt = 0{\cdot}26$, or

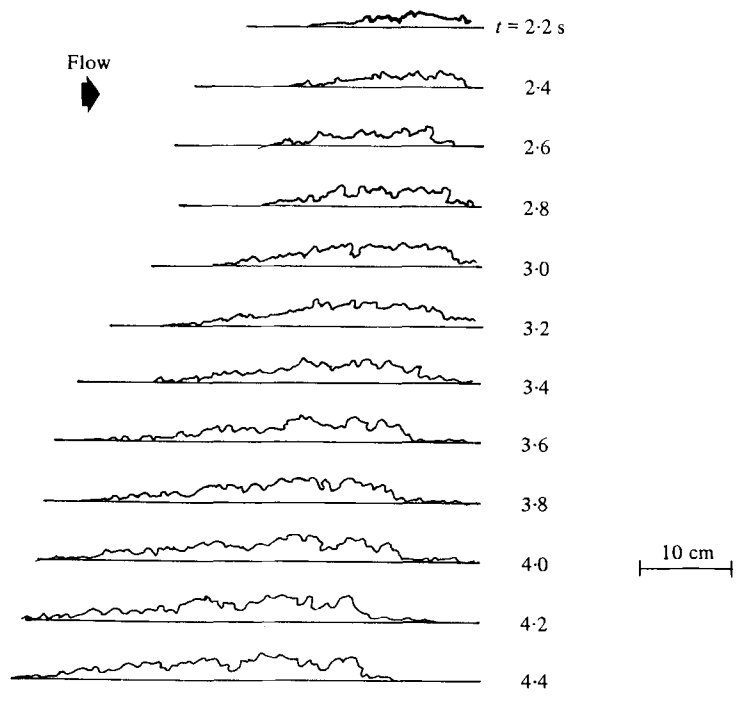

(*b*)

FIGURE 15(*b*). For legend see p. 89.

26 per cent of a Brunt–Väisälä period). It is known that wakes in stratified fluids begin to collapse after about a quarter of a Brunt–Väisälä period (Lin & Pao 1979). Apparently the influence of stratification on the dynamics of a turbulent spot is similar to the influence on turbulent wakes.

The stratification made it more difficult to maintain a flat sheet of laser light because of the index of refraction changes caused by the density fluctuations. In addition, a view of the turbulent spot was distorted, as evidenced by the defocusing in figure 14(*b*), since the light emitted by the fluorescent dye had to pass through the fluid with fluctuations in the index of refraction. Those effects became more pronounced with the increase in the intensity of stratification ($N > 0{\cdot}1$ Hz). Runs conducted at progressively larger values of Brunt–Väisälä frequency were more difficult to analyse because of the distortion effects described. However, it was clear that increasing the Brunt–Väisälä frequency increased the suppression of the vertical growth of a turbulent spot.

The stratification did not seem to affect the spanwise growth of a turbulent spot, as estimated by the maximum angle subtended by the spot measured from its virtual origin. This angle was typically 10°, the same as that for the homogeneous case. However, due to collapse, it did affect the lateral spread of the head of the spot, causing it to be somewhat wider and flatter than for the non-stratified case. It is not clear how the overall shape of an 'old' spot, i.e. one that has existed for several Brunt–Väisälä periods, would be modified.

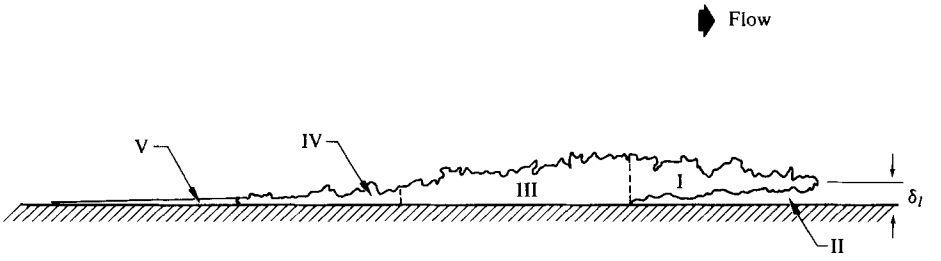

FIGURE 16. Schematic view of an x–y cut through the turbulent spot.

4. Concluding remarks

Turbulent spots evolving in a laminar boundary layer on a nominally zero pressure gradient flat plate were visualized using novel visualization techniques that utilized fluorescent dye and a laser. The extra degree of freedom provided by using fluorescent dye was found to be quite effective in revealing the structure of a turbulent spot. To elucidate the manner in which the spot (or any turbulent region in an unstable laminar boundary layer) spreads laterally, a turbulent wedge, generated by introducing a roughness element into the unstable laminar boundary layer, was investigated both visually and with probe measurements.

It was found that the spot grew normal to the plate by classical turbulent entrainment, in much the same way that a turbulent boundary layer grows. However, the growth in the spanwise direction, which has a rate of roughly an order of magnitude larger than the growth rate normal to the plate, was not due to classical entrainment. Our results strongly suggest that the spanwise growth may be due to a destabilization process, as suggested by Corrsin & Kistler (1955). We term this process *growth by destabilization*, which manifests itself as follows: the turbulent eddies within the spot appear to induce perturbations into the surrounding unstable laminar boundary layer which rapidly grow and break down, forming new turbulence, without ever being in direct contact with the older turbulence.

No dominant vortex was observed in the visualizations, but instead the spot appeared to be composed of a collection of somewhat independent, random eddies, much as in a turbulent boundary layer.

A qualitative picture of the different dynamic regions of a spot is given in figure 16. It shows a schematic of an x–y cut through a sector of the spot (excluding the region near the wingtips). Region I, the head of the spot, is a result of turbulent fluid being swept over the laminar boundary layer. This region, being cut off from the turbulence near the plate and its associated generation processes (e.g. bursting), appeared fairly passive, in agreement with the measurements of Cantwell *et al.* (1978).

However, region I exhibits a pronounced overhang over region II, the laminar boundary layer below and ahead of the spot. In region II, perturbations due to the presence of the spot are felt upstream of the spot, but the breakdown to turbulence does not occur until the spot rides over this laminar region. It is not yet clear whether the perturbation and growth of the instability ahead of the spot are important, or whether the flow is driven unstable by the overhang region. The front of the spot appears to be growing mostly in region II, as the laminar boundary layer breaks

down. New turbulence is thus added to the lower front part of the spot, which is again consistent with the measurements of Cantwell *et al.* (1978).

Region III appears to be dynamically very similar to a classic boundary layer over a flat plate. The growth rates normal to the plate are about the same for the turbulence in region III and for a turbulent boundary layer. Furthermore the entrainment of nonturbulent fluid in planes normal to the wall appeared to involve large-scale eddies in a gulping process similar to a fully developed turbulent boundary layer.

As the streamwise mean shear acts upon the spot, it exposes a region of fluid, region IV, which was originally in the lower part of a turbulent-boundary-layer-like flow, but which is now left to interact with the oncoming laminar boundary layer and the external potential flow. This turbulent fluid is still rather active, and quickly begins entraining the fluid above it. This produces the growth of the spot in the rear as observed in x, z planes (see figure 3).

Finally, region V denotes the 'calmed' region following the spot. The streaks of dye aligned with the streamwise direction seem to be the dominant characteristics in the visualization results shown here and by others. It is commonly believed that these streaks are the result of streamwise vortices lying near the wall which raise the dye seeping into the calmed region of the spot (observed on the extreme left in figure 2).† However, this region remains laminar, possibly due to the stable velocity profile in the region.

Cross-sections of the spot off the centre-line are similar to that sketched in figure 16, except the relative lengths of the different regions will vary in the spanwise direction. In the region near the wingtips, it is not clear that an overhang exists. Although it may not exist, the ciné films do show that the flow approaching the wingtips becomes highly contorted and breaks down as it passes into the vicinity of the wingtips in a manner similar to that seen at other locations around the spot.

The detailed mechanism of how the turbulence induces fluctuations into the unstable boundary layer is not known. However, figures 4, 6 and 7 show that this may be partly accomplished by the 'massaging' action of the turbulent overhang, i.e. turbulent eddies in region I of figure 16 at $y \approx \delta_l$, which at a fixed streamwise location precede the occurrence of turbulence near the wall. The actual extent of the overhang is difficult to estimate from the visualization results; however, both Wygnanski *et al.* (1976) and Cantwell *et al.* (1978) reported that it is many laminar-boundary-layer thicknesses on the centre-line. Cantwell *et al.* also showed that the first detectable velocity change preceding the spot occurred approximately 25 laminar-boundary-layer thicknesses ahead of the initial occurrence of the overhang; thus the spot is indeed felt at considerably removed distances within the unstable laminar boundary layer.

Since the laminar boundary layer is unstable to Tollmien–Schlichting waves, it is tempting to suggest that the induced disturbances will grow accordingly. This does not seem to be the case, however. The wavelengths observed in figure 4 of 1–2 laminar-boundary-layer thicknesses are small for Tollmien–Schlichting waves. In addition, the growth rates of the disturbances seem too large when compared with the linear theory. However, since the laminar boundary layer near the spot is distorted

† It is likely that these streaks are just the remnants of the sublayer streaks in Regions III and IV.

from the Blasius profile, a more detailed calculation and comparison is required before the linear Tollmien–Schlichting mechanism can be eliminated.

Whenever sinuous motion occurred in the dye lines upstream of the spot, usually only 1–2 wavelengths were visible as seen in figure 4. However, since a large amplitude is needed before they can be seen, it is possible that these oscillations were part of a longer wave-train. The spanwise extent of the oscillations was nominally one wavelength. As indicated earlier, the growth rate of the oscillations prior to breakdown was quite large. This evidence has led to the speculation that the observed oscillations may be similar to those observed by Klebanoff *et al.* (1962) just prior to breakdown in an unstable laminar boundary layer. That is, the oscillations associated with the 'spike' had a wavelength of roughly one boundary-layer thickness, were of limited spanwise extent and exhibited only a few oscillations before breaking down into complete chaos, i.e. turbulence. Because Klebanoff *et al.* have a more controlled experiment, their observed oscillations and breakdown were more repeatable than in the present experiment. That notwithstanding, the similarities between the two is highly suggestive that similar mechanisms may be responsible for the observed breakdown in both experiments.

The evidence suggests that the spanwise growth is governed by the disturbance field of the turbulent eddies in the vanguard of the spot and the stability characteristics in the surrounding laminar boundary layer. As a turbulent eddy grows to elevations outside the laminar boundary layer, it is carried downstream over the unstable laminar regions by the free stream. The velocity field of the eddy induces disturbances into the unstable laminar boundary layer which propagate and grow according to the dominant instability mechanism and ultimately break down into turbulence. Thus the leading edge of the spot is not a convected interface, but is a locus of points where the fluctuations have broken down into turbulence.

This hypothesis is consistent with the results from the dilute polymer solution experiments. Since less dye seemed to have been removed from the plate under these conditions, the polymers seemed to have suppressed the turbulence intensity. Also the lateral growth rate was reduced by about 15 per cent, resulting in a more elongated spot. The experiments confirm that the polymer effects are closely associated with wall phenomena. For while the addition of polymer seems to modulate the growth by destabilization mechanisms, it doe not seem to affect the entrainment mechanism.

Stratification was also used to modulate the turbulent spot. The stratification inhibited the vertical growth of the turbulent spot. The effect is more pronounced as the density gradient, and hence the Brunt–Väisälä frequency, is increased. The head of the spot collapsed after about $\frac{1}{4}$ Brunt–Väisälä period, much the same as a wake collapse in a stratified fluid. There did not seem to be any effect on the spanwise growth as measured by the spreading angle of the spot.

The final picture which emerges from this set of experiments is that the growth of turbulent spots in the spanwise direction is an order of magnitude greater than the growth normal to the plate, and that the spanwise growth is by destabilization of the surrounding unstable laminar boundary layer. Although a conceptual model is suggested which correlates the present observations, further work is required to understand fully this new growth mechanism.

An earlier, but less complete, version of this work has appeared in the proceedings

of the IUTAM Symposium on Laminar–Turbulent Transition (Gad-el-Hak, Blackwelder & Riley 1979). This work is sponsored by the Air Force Office of Scientific Research, United States Air Force, under contract F49620-78-C-0062. The wind tunnel data were obtained with the support of the U.S. Army Research Office, under Grant DAAG29-76-G0297. Partial support was also obtained from the National Aeronautics and Space Administration, Ames Research Center. The authors would like to acknowledge the valuable help of S. Corrsin, M. Gaster, P. Klebanoff, H.-T. Liu, M. Morkovin, L. Ormand, M. Weissman & I. Wygnanski.

REFERENCES

ANDERS, J. B. & BLACKWELDER, R. F. 1980 Longitudinal vortices in a transitioning boundary layer. *Proc. IUTAM Symp. on Laminar–Turbulent Transition*. Springer.

BERMAN, N. S. & GEORGE, W. K. 1974 Onset of drag reduction in dilute polymer solutions. *Phys. Fluids* **17**, 250.

BERTSHY, J. R. & ABERNATHY, F. H. 1977 Modifications to laminar and turbulent boundary layers due to the addition of dilute polymer solutions. *Proc. 2nd Int. Conf. on Drag Reduction, Cambridge, England.*

BLACKWELDER, R. F. & KOVASZNAY, L. S. G. 1972 Time scales and correlations in a turbulent boundary layer. *Phys. Fluids* **15**, 1545.

BURGERS, J. M. 1924 The motion of a fluid in the boundary layer along a plane smooth surface. *Proc. 1st Int. Cong. of Applied Mech., Delft*, p. 113.

CANTWELL, B., COLES, D. & DIMOTAKIS, P. 1978 Structure and entrainment in the plane of symmetry of a turbulent spot. *J. Fluid Mech.* **87**, 641.

CHARTERS, A. C. 1943 Transition between laminar and turbulent flow by transverse contamination. *N.A.C.A. Tech. Note* no. 891.

CHEN, C.-H. P. & BLACKWELDER, R. 1978 Large-scale motion in a turbulent boundary layer: a study using temperature contamination. *J. Fluid Mech.* **89**, **1**.

COLES, D. & BARKER, S. J. 1975 Some remarks on a synthetic turbulent boundary layer. In *Turbulent Mixing in Nonreactive and Reactive Flows* (ed. S. N. B. Murthy), p. 285. Plenum.

CORRSIN, S. & KISTLER, A. L. 1955 Free-stream boundaries of turbulent flows. *N.A.C.A. Rep.* no. 1244. (Supersedes *N.A.C.A. TN* 3133.)

DRYDEN, H. L. 1934 Boundary layer flow near flat plates. *Proc. 4th Int. Cong. of Applied Mech., Cambridge, England*, p. 175.

DRYDEN, H. L. 1936 Airflow in the boundary layer near a plate. *N.A.C.A. Rep.* no. 562.

DRYDEN, H. L. 1939 Turbulence and the boundary layer. *J. Atmos. Sci.* **6**, 85, 101.

ELDER, J. W. 1960 An experimental investigation of turbulent spots and breakdown to turbulence. *J. Fluid Mech.* **9**, 235.

EMMONS, H. W. 1951 The laminar–turbulent transition in a boundary layer. *J. Aero. Sci.* **18**, 490.

FALCO, R. E. 1977 Coherent motions in the outer region of turbulent boundary layer. *Phys. Fluids* **20**, S124.

FIEDLER, H. E. & HEAD, M. R. 1966 Intermittency measurements in a turbulent boundary layer. *J. Fluid Mech.* **25**, 719.

GAD-EL-HAK, M., BLACKWELDER, R. F. & RILEY, J. J. 1979 A visual study of the growth and entrainment of turbulent spots. *Proc. IUTAM Symp. on Laminar–Turbulent Transition, University of Stuttgart*, p. 297. Springer.

GASTER, M. 1975 A theoretical model of a wave packet in the boundary layer on a flat plate. *Proc. Roy. Soc.* A **347**, 271.

GASTER, M. 1978 The physical processes causing breakdown to turbulence. *12th Naval Hydrodynamics Symposium, Washington, D.C.*, p. 22.

GASTER, M. & GRANT, I. 1975 An experimental investigation of the formation and development of a wave packet in a laminar boundary layer. *Proc. Roy. Soc.* A **347**, 253.

HAMA, F. R., LONG, J. D. & HAGARETY, J. C. 1957 On transition from laminar to turbulent flow. *J. Appl. Phys.* **28**, 388.

KLEBANOFF, P. S., TIDSTROM, K. D. & SARGENT, L. M. 1962 The three-dimensional nature of boundary layer instability. *J. Fluid Mech.* **12**, 1.

KOVASZNAY, L. S. G., KOMODA, H. & VASUDEVA, B. R. 1962 Detailed flow field in transition. *Proc. Heat Transfer and Fluid Mech. Inst.*, p. 1. Stanford University Press.

LIN, J.-T. & PAO, Y.-H. 1979 Wakes in stratified fluids. *Ann. Rev. Fluid Mech.* **11**, 317.

MEYER, K. A. & KLINE, S. J. 1961 A visual study of the flow model in the later stages of laminar–turbulent transition on a flat plate Mech. Eng. Dept., Stanford University, Rep. no. MD-7.

MORKOVIN, M. V. 1969 Critical evaluation of transition from laminar to turbulent shear layers with emphasis on hypersonically travelling bodies. *Flight Dyn. Lab. Rep.* no. AFFDL-TR-68-149.

SCHLICHTING, H. 1933 Zur Entstehung der Turbulenz bei der Plattenströmung. *Z. angew. Math. Mech.* **13**, 171.

SCHUBAUER, G. B. & KLEBANOFF, P. S. 1956 Contributions on the mechanics of boundary layer transition. *N.A.C.A. Rep.* no. 1289.

SCHUBAUER, G. B. & SKRAMSTAD, H. K. 1948 Laminar boundary layer oscillations on a flat plate. *N.A.C.A. Rep.* no. 909.

TOLLMIEN, W. 1931 The production of turbulence. *N.A.C.A. TM* 609.

TOWNSEND, A. A. 1976 *The Structure of Turbulent Shear Flow.* Cambridge University Press.

VAN ATTA, C. W. & HELLAND, K. N. 1980 Exploratory temperature-tagging measurements of turbulent spots in a heated laminar boundary layer. *J. Fluid Mech.* **100**, 243.

VAN DER HEGGE ZIJNEN, B. G. 1924 Measurements of the velocity distribution in the boundary layer along a plane surface. Thesis, Delft.

WYGNANSKI, I., HARITONIDIS, J. H. & KAPLAN, R. E. 1979 On Tollmien–Schlichting wave packet produced by a turbulent spot. *J. Fluid Mech.* **92**, 505.

WYGNANSKI, I., SOKOLOV, M. & FRIEDMAN, D. 1976 On a turbulent 'spot' in a laminar boundary layer. *J. Fluid Mech.* **78**, 785.

ZILBERMAN, M., WYGNANSKI, I. & KAPLAN, R. 1977 Transitional boundary layer spot in a fully turbulent environment. *Phys. Fluids Suppl.* **20**, 258.

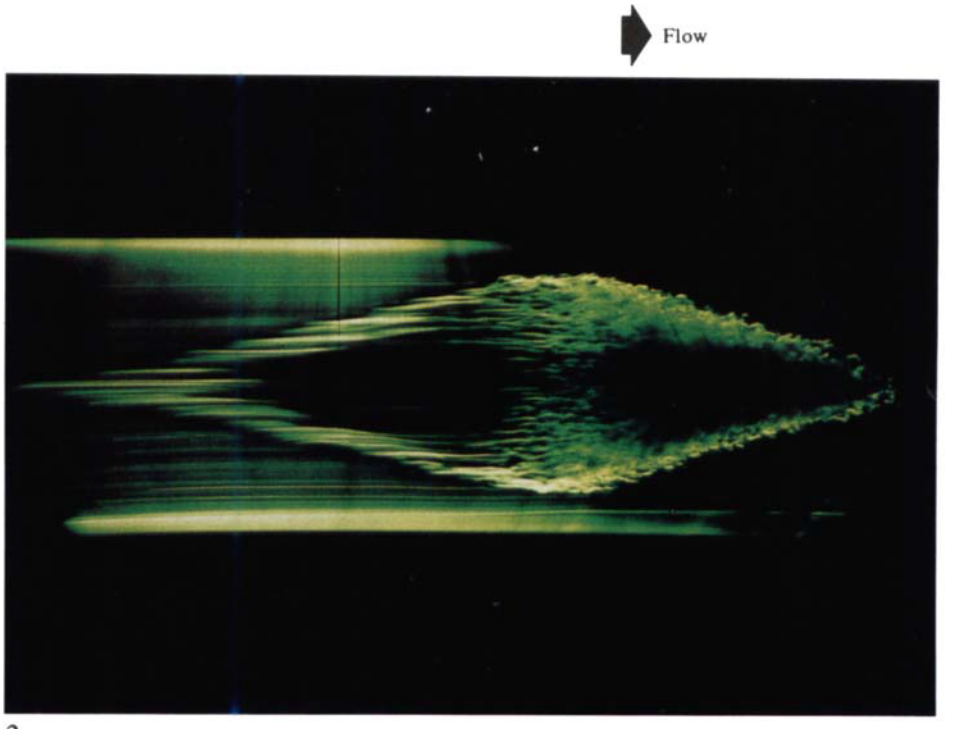

2

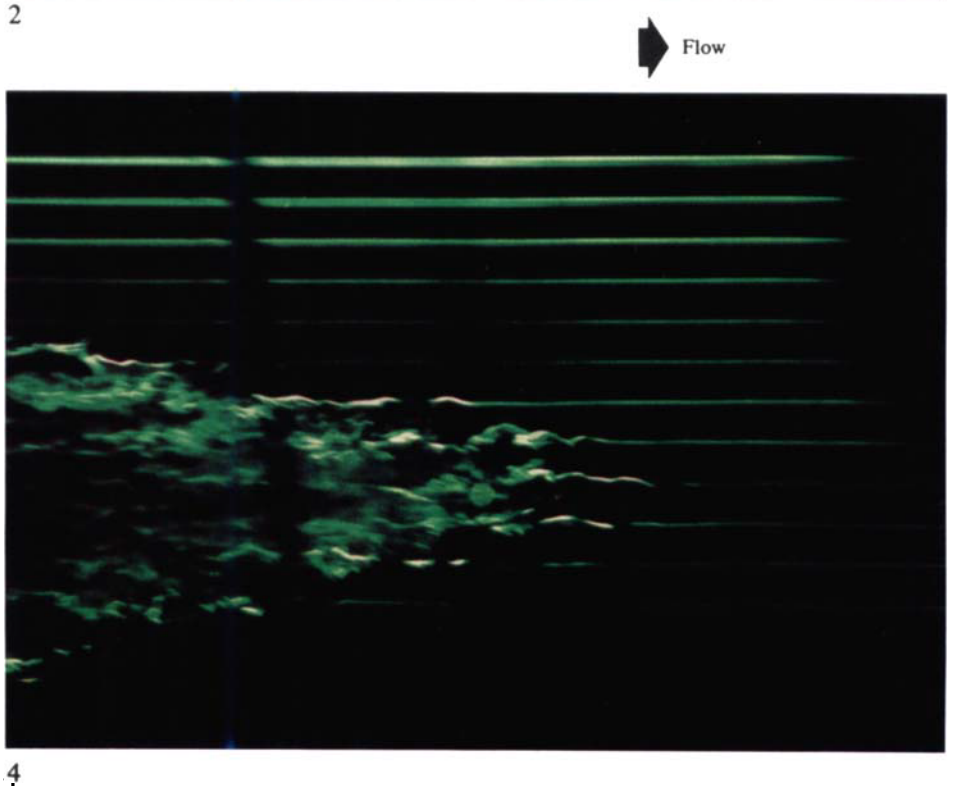

4

FIGURE 2. A plan view of the turbulent spot at $y = 0$.

FIGURE 4. Plan view of the spot at $y = 0{\cdot}1$ cm. The dye lines fixed in the fluid undergo large-amplitude oscillations before being overtaken by the spot.

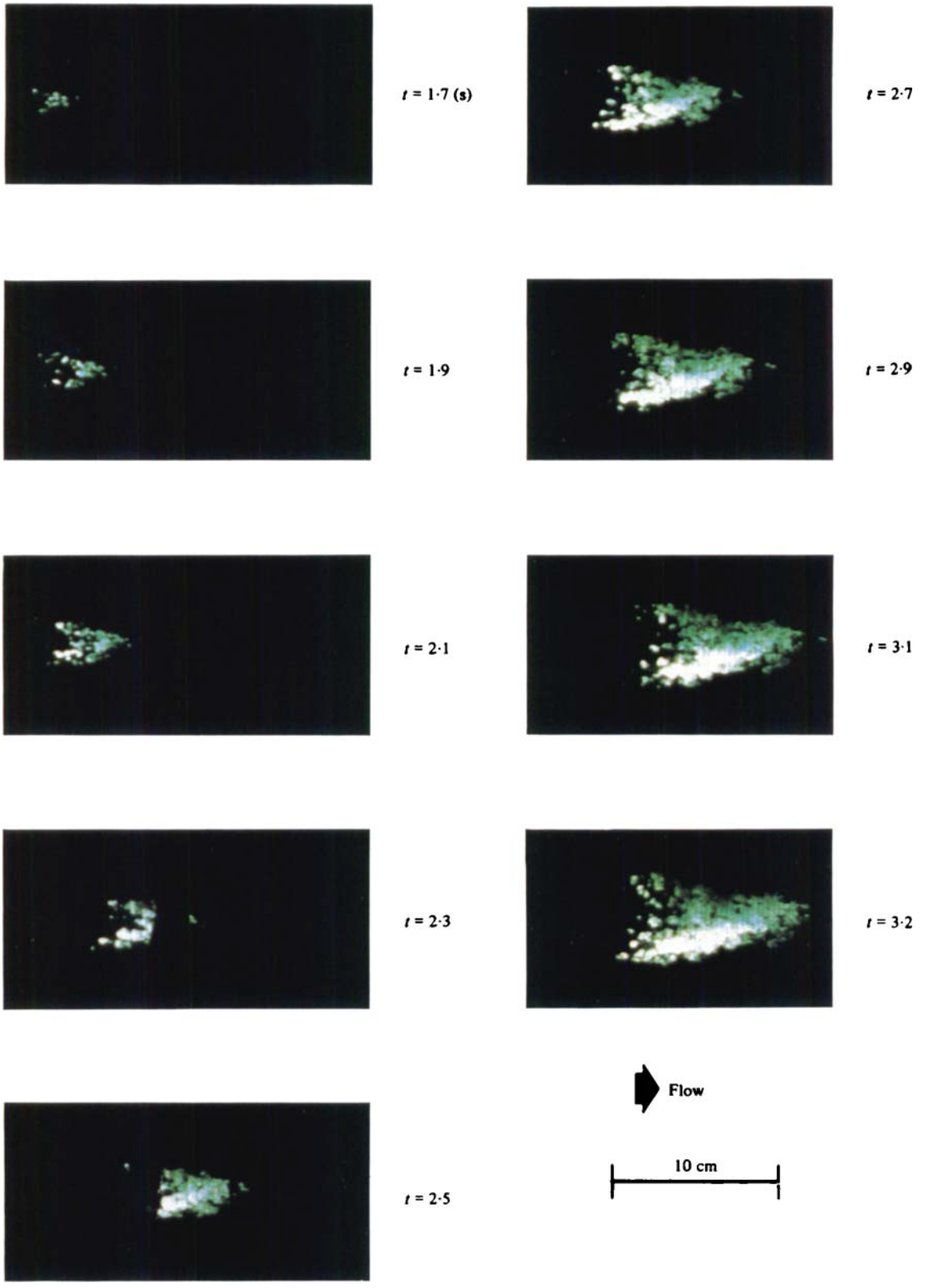

FIGURE 3. Sequence of plan views at $y = 1{\cdot}3$ cm, illustrating the growth of the spot. The time since the spot generation is indicated to the right.

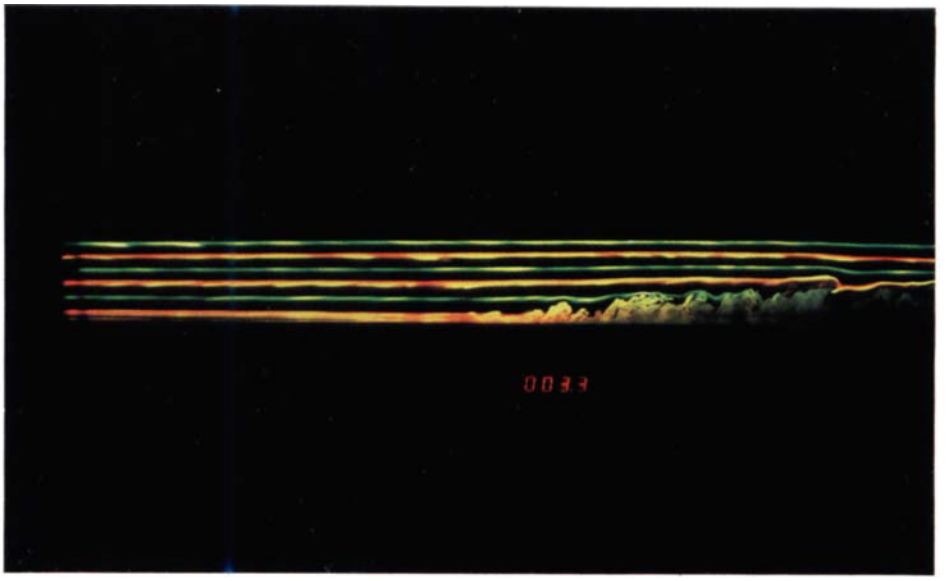

(*a*)

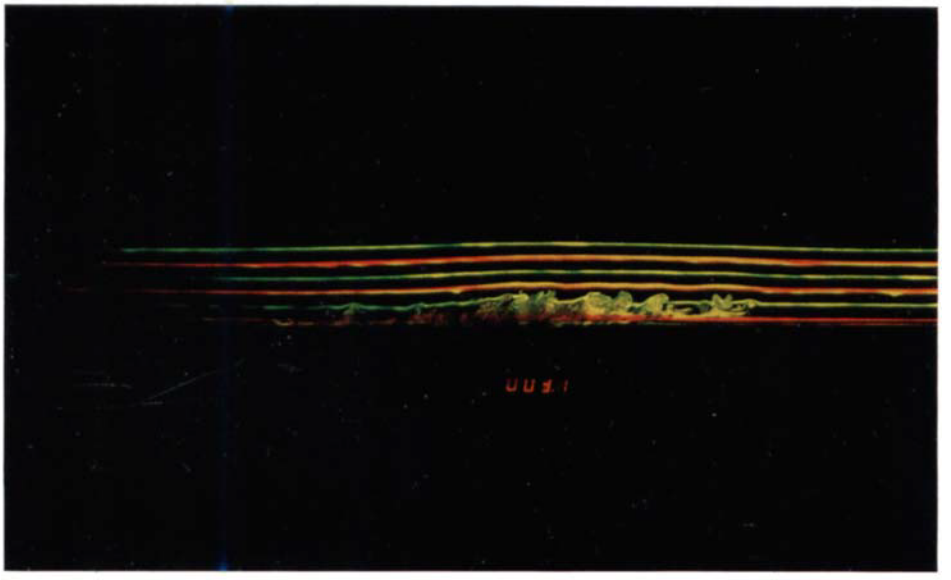

(*b*)

FIGURE 5. Cross-sectional view in the x, y plane of the turbulent spot at two different spanwise locations. (*a*) $z = 0$; (*b*) $z = 6$ cm.

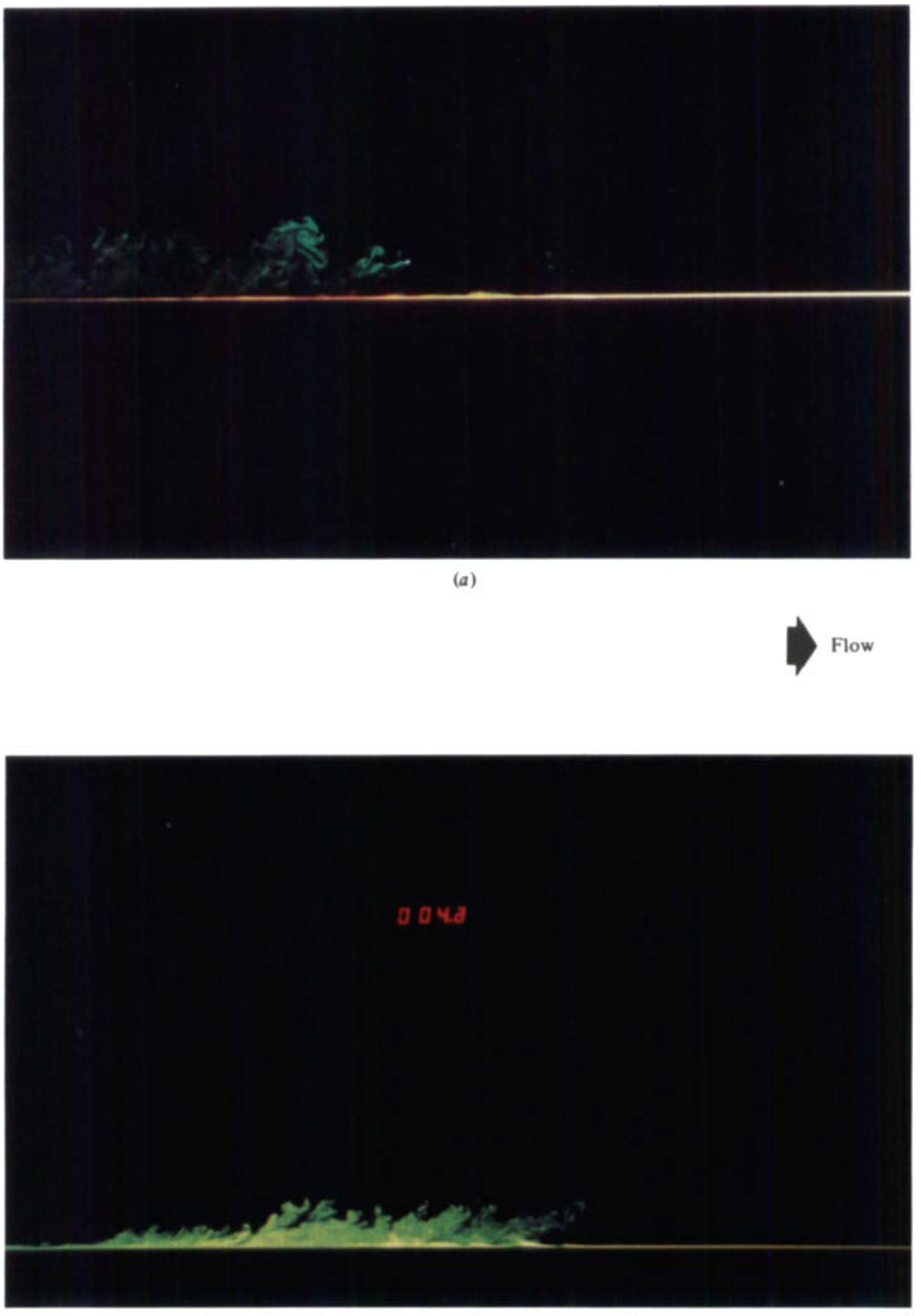

FIGURE 6. Cross-sectional view in the x, y plane of a turbulent spot. (*a*) $z = 0$; (*b*) $z = 6$ cm.

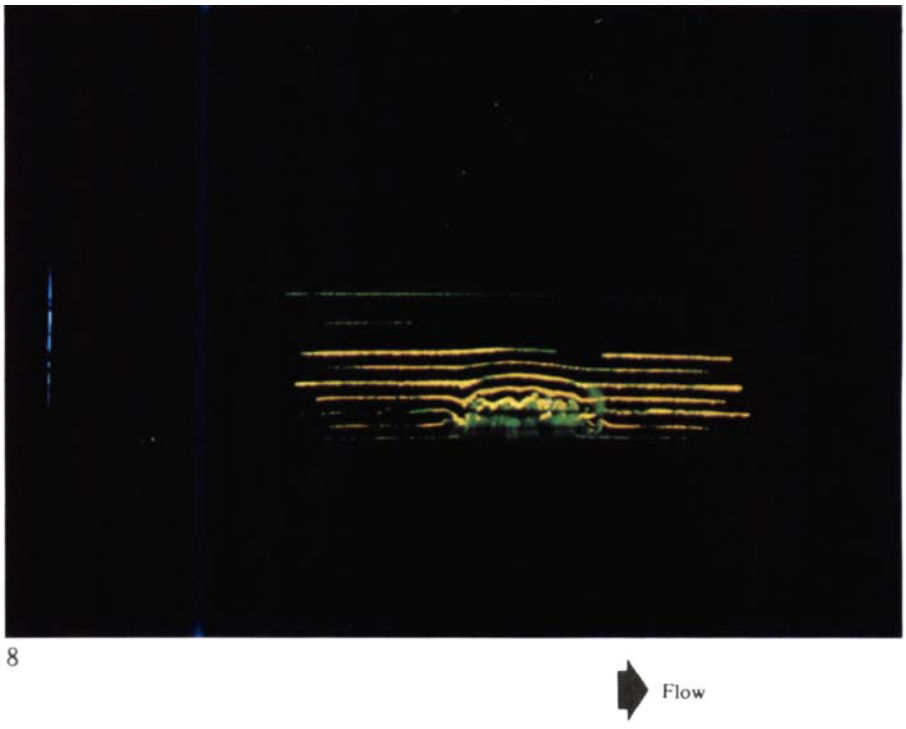

FIGURE 8. Spanwise section of the spot in the y, z plane.

FIGURE 13. Plan view of a turbulent spot in 50 p.p.m., WSR-301 solution. Sheet of light at $y = 0$, and plate is towed at 60 cm s^{-1}.

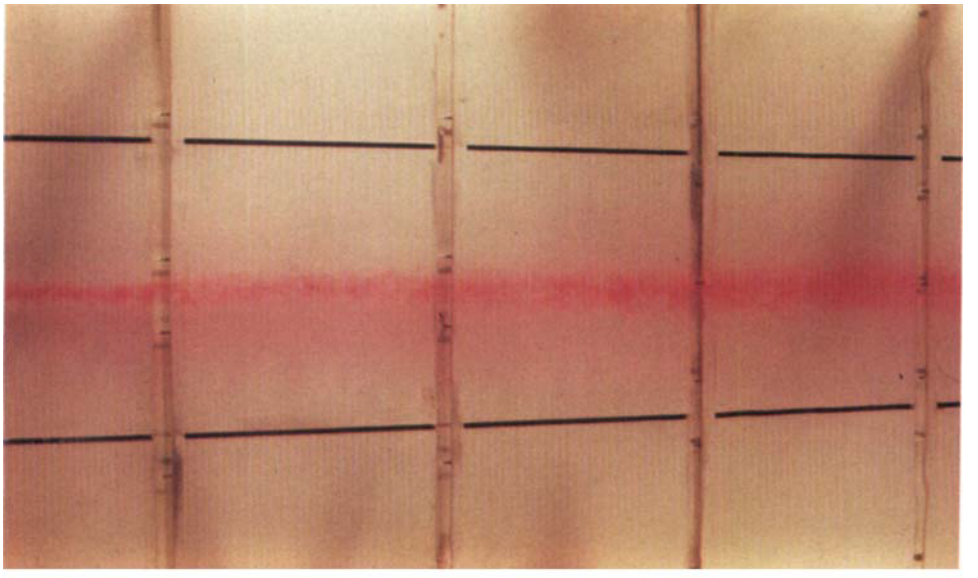

(*a*)

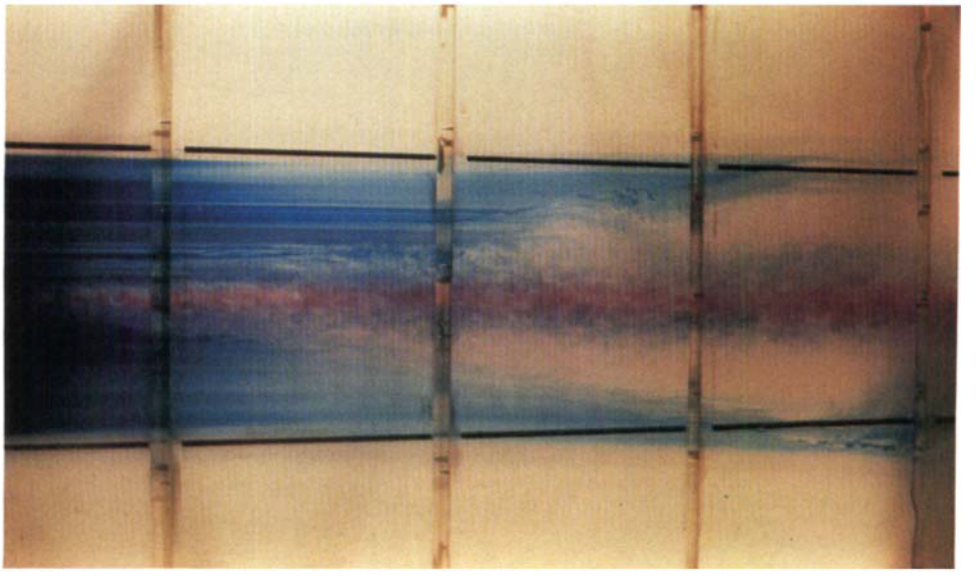

(*b*)

FIGURE 9. Effects of a roughness element in an unstable laminar boundary layer. The cylinder is located at $R_x = 9 \times 10^4$. (*a*) Dye emanates from the cylinder only. (*b*) Dye is also allowed to seep from the spanwise slot.

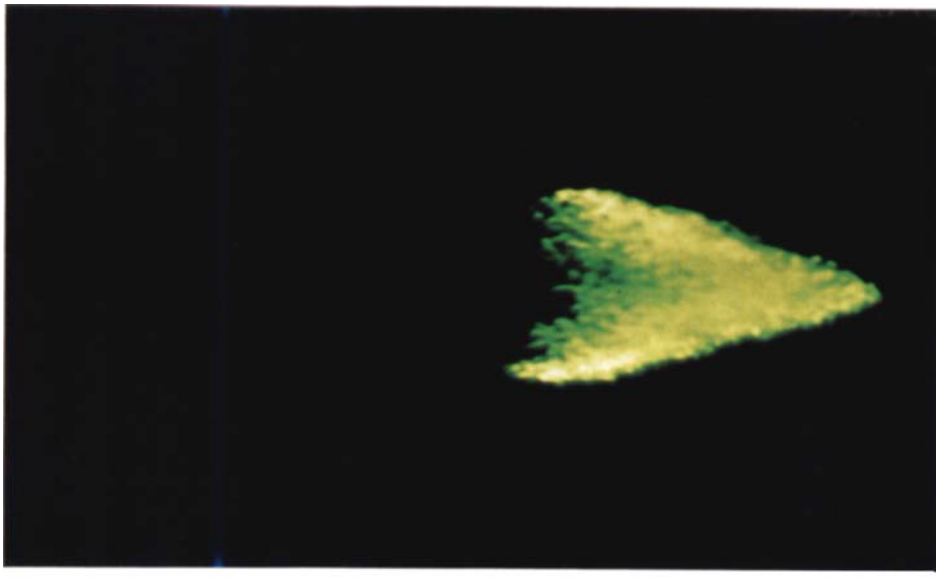

(*a*)

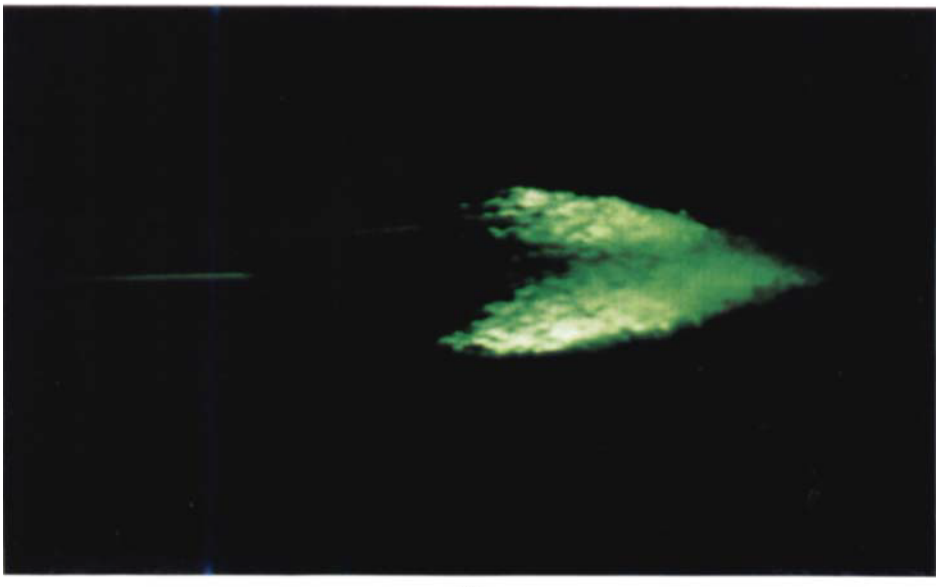

(*b*)

FIGURE 12. Plan view of a turbulent spot. Sheet of light is at $y = 3$ mm, and plate is towed at 40 cm s^{-1}. (*a*) Pure water, (*b*) 50 p.p.m. WSR-301 solution.

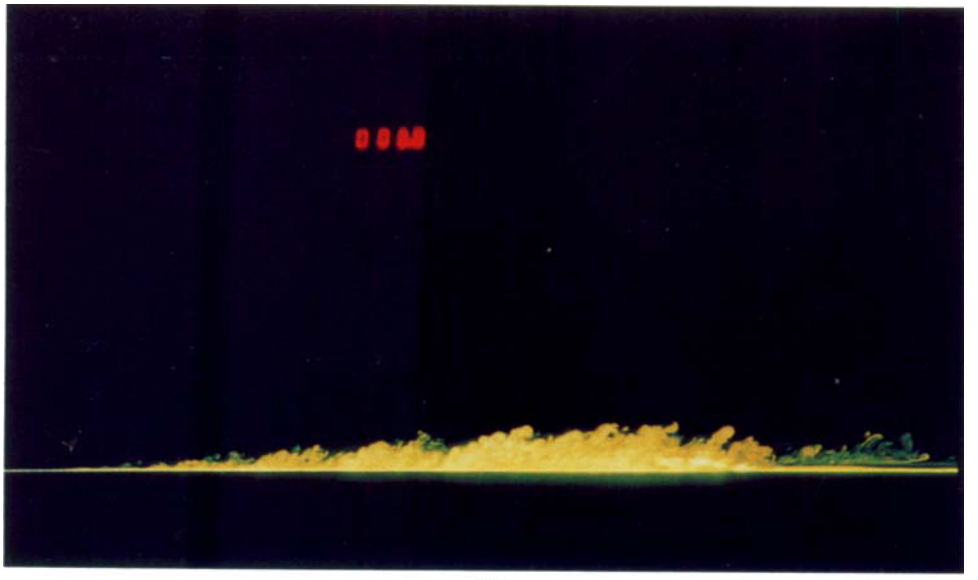

(*a*)

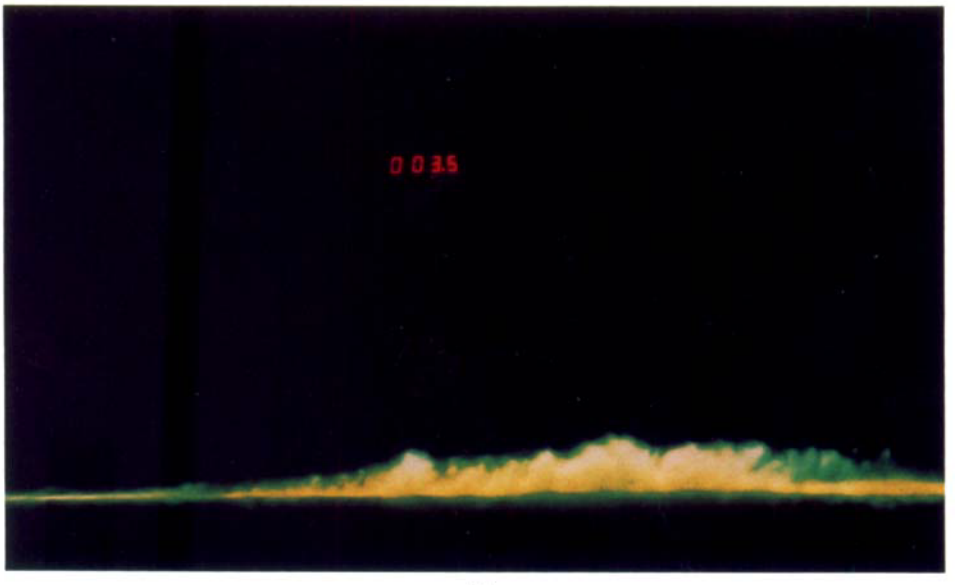

(*b*)

FIGURE 14. Cross-sectional view in the x, y plane. Sheet of light at $z = 0$ cm, and plate is towed at 40 cm s^{-1}. (*a*) Homogeneous fluid. (*b*) Stratified fluid, $N = 0{\cdot}1$ Hz.